Blockage Arrangements Modelling in Indoor Wireless Networks: A Comparative Study

Viktor Stoynov[1] and Zlatka Valkova-Jarvis[2]

Abstract – **In this work, the performance of indoor users' throughput is studied through the abstract modelling of walls. A more realistic blockage object arrangement is compared with existing abstract-modelled blockage arrangements to demonstrate its improved representation of real-life scenarios. Ten different scenarios are defined, combining different wall layouts and transmitter dispositions. The scenarios represent possible real working environment sites and are experimentally tested for different numbers of receivers.**

Keywords – **Indoor environment, wireless communications, blockage modelling, user throughput**

I. Introduction

One of the main problems facing telecommunication networks is how to provide an excellent service to users located at the periphery of the serving cell. These users are subject to significant interference from neighbouring base stations and, in the case of wireless indoor environments, from adjacent transmitters (*Tx*). One major obstacle in enclosed spaces is the wall layout: walls, as blockage objects, mitigate interference but also cause the signal to deteriorate, thus worsening the quality of the mobile services provided. Good indoor coverage depends to a large extent on the femtocells' location. The signals from non-serving transmitters permeate the wall and fade easily, hence they are not a source of interference.

The modelling of indoor obstacles is often neglected and the enormous influence of wall layout on signal propagation is thus overlooked in the research. Some recent works [1], [2], [3] have presented and investigated different wall generation models of indoor communication environments, and considered the major parameters of signal obstacles, such as length, attenuation level, density allocation, etc. Analytical expressions of the average attenuation of signals passing through walls are derived and system-level simulations performed to demonstrate the impact of the walls and transmitter devices arrangement on the Signal-to-Interference Ratio (SIR) and users' throughput.

In this paper a new, more realistic, abstract-modelled wall layout is investigated. It demonstrates clear advantages when compared experimentally to previously-developed similar abstract models. Furthermore, ten scenarios, consisting of four different types of wall distributions and free indoor space propagation, are evaluated and compared. The abstract wall generation methods use the same wall density, aiming to achieve clear conclusions after the direct comparison of users' throughputs. The experimental set uses the same enclosed space (Region of Interest - RoI), number of *Tx*, transmitter distance and power, while the number of users (receivers - *Rx*) varies. Using the same amount of physical resources in each scenario while increasing the number of users leads to a decrease in average user throughput.

Viktor Stoynov[1] and Zlatka Valkova-Jarvis[2] are with the Faculty of Telecommunications at Technical University of Sofia, Bulgaria, E-mails: {vstoynov, zvv}@tu-sofia.bg.

II. System Model

A. Abstract wall layouts generation methods

In this work, four methods for wall arrangement are considered (Fig. 1). The first wall generation method is based on a Boolean scheme, where the positions of the centre points of the walls are randomly distributed according to a Poisson Point Process (PPP) of density λ. The lengths of the walls follow arbitrary distribution $f_L(l)$. The disposition of the walls is either parallel or at right-angles, which defines a two-state wall layout, realised when the angle between any two walls is a binary choice – $\{0; \pi/2\}$. This abstract wall generation method is denoted as **[binary]** (Fig. 1a).

The wall distribution, generated by a Manhattan grid of equidistantly-spaced walls is named **[regular]** (Fig. 1b). It is assumed that the walls are oriented perpendicularly to the coordinate axes. The space between every two adjacent parallel walls is set to a constant Δ. This distance is calculated based on the dimensions of the considered RoI and is related to the average wall length $E[L]$ and wall density parameter λ: $\Delta=2/\lambda E[L]$. Geometrically, the RoI is a rectangle or square with sides whose length is both an integer and a multiple of Δ. In order to achieve different realisations of the **[regular]** wall layout, Δ might be randomly shifted by δ_x in the *x*-axis and by δ_y in the *y*-axis.

The third abstract, but more realistic, wall generation method is obtained by two Manhattan Line Processes (MLP) and is named after it - **[MLP]** (Fig.1c). This method is very similar to the **[regular]**, but differs in that the wall distance Δ is not a constant but a variable.

The fourth method of blockage arrangement named Realistic Indoor Environment Generator - **[RIEG]** (Fig.1d) is designed as a simple generation tool of indoor environments. It consists of positioning rectangles in a predefined area – RoI. The coordinates of the starting point of each rectangle are selected randomly. The sides of the rectangle are then plotted, ensuring that the rectangle remains within the RoI. The total length of the walls takes into account the value of the wall density parameter. Hence, different methods for wall arrangement can be compared. The confined spaces, resulting from the rectangles' distribution, achieve a more realistic indoor design compared to the other three methods.

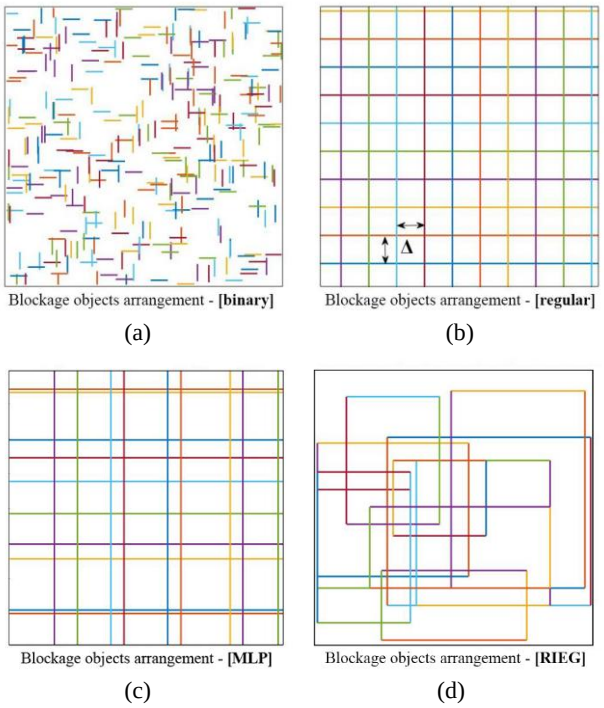

Fig.1. Generated wall maps for (a) **[binary],** (b) **[regular],** (c) **[MLP]** and (d) **[RIEG]** cases

There are also scenarios where no walls are distributed – **[free space]**. Thus, the experimental *results* can show how the existence of walls affects the level of user throughput.

B. Transmitter and receiver location

Four *Txs* in the indoor system model are located in the vertices of a square with side-length *R*, denoted as **[square]** in the scenarios' descriptions (Fig. 2a). When the **[square]** constellation of transmitters is rotated by an angle of $\pi/4$, the alternative transmitters' disposal is obtained. It is labelled as **[rhomboid]** and is shown in Fig. 2b. These two transmitter setups simplify the theoretical analysis of the system interference.

The receivers are located at the cell edge, at a constant distance of *R*/2 from the closest transmitter. This transmitter is denoted as the desired transmitter – (*dTx*). The other three transmitters are assumed to be sources of interference ($iTx_{1\div3}$). The position of each receiver is determined by its polar coordinates ($R/2$, Φ), measured against the nearest transmitter. The angle Φ ranges from 0 to $\pi/2$ (Fig. 2).

III. ANALYTICAL MODEL

The downlink signal is assumed to experience attenuation due to the wall blockages, distance-dependent path loss and small-scale fading. The path loss law *l(d)* is defined in [4]. The attenuation due to the walls is determined by summing the attenuation of each wall.

In the models considered in this work, the blockages are defined as two-dimensional objects, and the investigated wireless network is designed to be interference limited.

One of the most important parameters is the average number of blockages $E[K]$ that obstruct the path with length *d* between the *Tx* and the *Rx*. For the **[binary]** case, this can be expressed as:

$$E[K] = \lambda E[L] d \frac{\left(|\sin(\phi)| + |\cos(\phi)|\right)}{2}. \quad (1)$$

where ϕ denotes the angle of the link between transmitter and receiver against the *x*-axis.

It is clear that the average number of blockages $E[K]$ located between a *Tx* and a *Rx* is directly proportional to the average length of these wall objects $E[L]$.

For the **[regular]** case, $E[K]$ is calculated as:

$$E[K] = N_x + N_y + p_x + p_y, \quad (2)$$

where N_x and N_y denote the number of walls without random shifts δ_x or δ_y, while p_x and p_y are the number of new walls, required to preserve the average wall density, after a random shifting is performed.

When the number of walls is set to K_i, the total attenuation of the signals in the area will be $\omega_i=\omega^{K_i}$. Although each wall may have a different attenuation, the experiments conducted here consider 10 dB fixed attenuation. Thus the SIR for one indoor user will be:

$$\gamma = \frac{P_0 h_0 l(d_0) \omega_0}{\sum_{i=1}^{3} P_i h_i l(d_i) \omega_i}, \quad (3)$$

where d_o is the distance between the receiver *Rx* and its serving (desired) transmitter *dTx*, P_0 is the transmit power of *dTx*, while P_i (i = 1, 2, 3) is the power of the interfering transmitters iTx_1, iTx_2 and iTx_3, respectively. h_0 and h_i denote the small-scale fading, d_i is the distance between the receiver and the $i^{\text{-th}}$ interfering transmitter and $l(d_0)$ and $l(d_i)$ are the path losses.

In [1] an analytic expression to approximate *geomean* (γ) for the **[binary]** case is derived. The average SIR is calculated by:

$$geomean(\gamma) \approx \int_{-\infty}^{\infty} \left(\frac{d}{d\delta} \left(1 - \prod_{i=1}^{3} \frac{1}{1 + \delta \frac{\overline{\omega}_i'}{\overline{\omega}_0} \frac{l(d_i)}{l(d_0)}} \right) \Bigg|_{\delta=t} \right) t \, dt. \quad (4)$$

$\overline{\omega}_i'$ provides an accurate approximation for *geomean* (ω_i) and is called effective wall attenuation.

For **[MLP]** the SIR is calculated by splitting the line-processes into the horizontal and vertical processes (Fig. 2a) [2]. For the **[square]** case, the SIR is calculated by:

$$\gamma = \frac{h_0 d_0^{-\alpha} \omega^{K_v + K_h}}{h_1 d_1^{-\alpha} \Omega_{sq\_1} + h_2 d_2^{-\alpha} \Omega_{sq\_2} + h_3 d_3^{-\alpha} \Omega_{sq\_3}}, \quad (5)$$

where

$$\Omega_{sq\_1} = \omega^{K_v' + K_h}; \quad \Omega_{sq\_2} = \omega^{K_v' + K_h'}; \quad \Omega_{sq\_3} = \omega^{K_v + K_h'}. \quad (6)$$

K_v and K_h are the wall counts between any user and the *dTx* and K'_v and K'_h are the wall counts between the user and the interfering transmitters iTx_1, iTx_2, iTx_3 (Fig. 2a). They all are Poisson Random Variables.

For the **[rhomboid]** case (Fig. 2b), the SIR is defined by the equation:

$$\gamma = \frac{h_0 d_0^{-\alpha} \omega^{K_v + K_h}}{h_1 d_1^{-\alpha} \Omega_{rh\_1} + h_2 d_2^{-\alpha} \Omega_{rh\_2} + h_3 d_3^{-\alpha} \Omega_{rh\_3}}, \quad (7)$$

where

$$\Omega_{rh\_1} = \omega^{K'_v + S(-\cos(\phi))K_v + K'_h}; \quad \Omega_{rh\_2} = \omega^{K_v + K'_h + K''_h}; \quad \Omega_{rh\_3} = \omega^{K''_v + S(-\cos(\phi))K_v + K'_h}. \quad (8)$$

K''_v and K''_h denote the wall counts between any user and the interferers iTx_1, iTx_2, iTx_3 as shown in Fig. 2b.

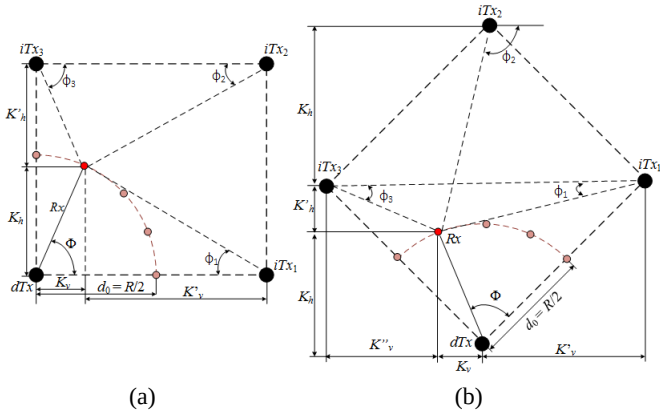

(a) (b)

Fig.2. Transmitters (*Tx*) and receivers (*Rx*) location (a) **[square]** and (b) **[rhomboid]**

IV. System-level simulations and results

A. Network design

The Vienna LTE-A system-level simulator [5] is an appropriate tool for the abstract modelling of the scenarios considered in this work. The results for users' throughput are obtained after 500 simulation runs, each with 200 identical transmission time intervals. The wall attenuation research conclusions are the result of 5000 simulations. The four transmitters are spaced a distance of R=40m apart, regardless of the pattern of their arrangement - **[square]** or **[rhomboid]**. Each *Tx* is defined as a femtocell with a transmit power of 100mW. The distance between the *dTx* and the receivers is set to 20m. The wall density is λ=0.05m^{-2}, the average wall length is $E[L]$=5m and the wall attenuation is set to 10 dB for each simulation. The experiments are conducted under the same conditions - the average number of walls, receivers and transmitters remaining constant for each simulation. The defined ten scenarios are simulated for two distinct numbers of users – 5 and 15.

Combining the location of the transmitters and wall layouts, the following ten scenarios are defined: **S1 = {[binary], [square]}**, **S2 = {[binary], [rhomboid]}**, **S3 = {[regular], [square]}**, **S4 = {[regular], [rhomboid]}**, **S5 = {[MLP], [square]}**, **S6 = {[MLP], [rhomboid]}**, **S7 = {[free space], [square]}**, **S8 = {[free space], [rhomboid]}**, **S9 = {[RIEG], [square]}**, **S10={[RIEG], [rhomboid]}.**

B. Average wall attenuation and user throughput results

The average wall attenuation and SIR can be analytically calculated only for the **[binary]** wall distribution. The **[regular]** wall pattern scenarios can only be examined using simulations. In [1] and [2] the wall attenuations for the different scenarios are determined. The **[binary]**, **[regular]** and **[MLP]** scenarios are analytically verified and it is shown that analytical results and simulation curves for the average attenuation level per transmitter match perfectly for both **[square]** and **[rhomboid]** transmitter layouts.

Fig. 3 and 4 show the average throughput of each user when two different numbers of *Rx* positions are used – 5 and 15 respectively. Investigations using a larger number of users are performed in [6] and clear conclusions are drawn.

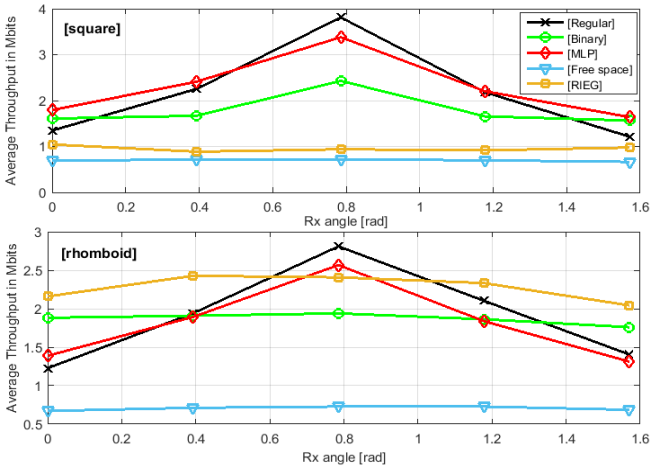

Fig.3. Average user throughput results for 5 users and **[square]** and **[rhomboid]** transmitter layouts

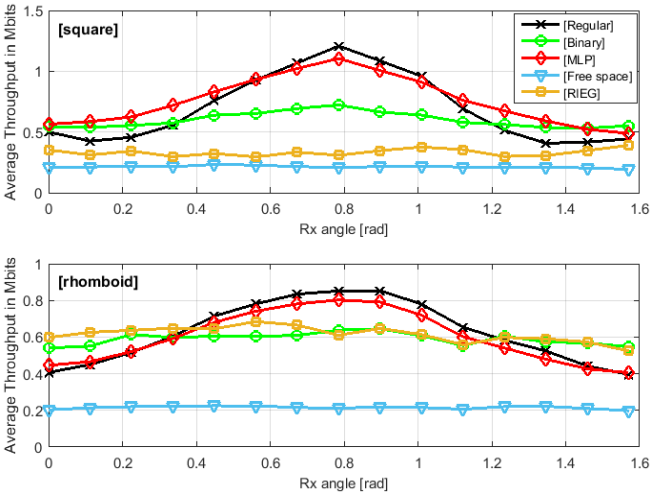

Fig.4. Average user throughput results for 15 users and **[square]** and **[rhomboid]** transmitter layouts

As anticipated, when **[free space]** scenarios are considered, the average throughput for each user dramatically decreases, which proves the important role of obstacles in interference mitigation. When comparing the simulation results for **[square]** and **[rhomboid]** transmitter layouts and an equal number of users, the same values of the throughputs are obtained. The location layouts of transmitters and receivers lose relevance when there are no walls – scenarios **S7** and **S8**. The angular collocation of the receiving and transmitting devices affects the wireless network performance only when direct visibility is impaired due to wall obstruction.

Apart from the users in the periphery of the femtocell, the graphs follow the same trend results regarding SIR as reported in [2]. The Manhattan grid-like wall arrangements, denoted as **[regular]** and **[MLP]**, show better performance compared to the **[binary]** and **[RIEG]** cases, no matter how many *Rx* positions are explored. This is caused due to the walls located along the *x*- and *y*-axis affecting the signal propagation between the *dTx* and the users to a much lesser extent. These walls, however, are able to suppress the interference from other transmitters ($iTx_{1\div3}$). Being a stochastic method, the distribution of the walls in **[binary]** is much more difficult to predict compared to **[regular]** and **[MLP]**.

In the case of **[MLP]** and **[regular]**, the **[square]** layout is characterised by lower interference compared to the **[rhomboid]** transmitters location, due to the different angular co-location of the walls to the desired transceiver. Walls parallel to the x- and y-axis remain invisible to *dTx*, which increases the throughput of the users located in positions $\Phi=0$ and $\Phi=\pi/2$. At these positions, the main sources of interference are the nearest distributed transmitters – iTx_1 and iTx_3 respectively (Fig. 2). The **[binary]** arrangement may provide fewer blockages to signal propagation, especially for user positions in $\Phi=0$ and $\Phi=\pi/2$, in contrast to the **[regular]** and **[MLP]** wall arrangements, which always contain obstacles between the *Rx* and the *dTx*. An increase of throughput is observed for *Rx* positions around $\Phi=\pi/4$, where the three interfering transmitters have an equally strong impact on the total interference. Clearly, the **[regular]** grid offers the best protection for users against interference.

It turns out that in the **[RIEG]** wall arrangement and **[square]** *Tx* locations, users receive nearly equal quality of service. Unlike the **[regular]** and **[MLP]** methods providing strictly determinate locations for the walls, when the **[RIEG]** layout is used the walls between users and transmitters are always random in number. In the **[rhomboid]** case, each wall can suppress the interference caused by $iTx_{1\div3}$, resulting in better coverage especially for users in the furthest positions compared to **[square]**. Logically, we may conclude that the more realistic the distribution of the walls used, the harder it becomes to predict their impact on user throughput. Obviously, due to the stochastic nature of wall arrangement the performance of **[RIEG]** is very similar to **[binary]**.

An interesting fact is that the **[MLP]** curves are very closely located to those for **[regular]** - something which is not observed in the figures for SIR. The reason for such behaviour is the identical number of walls for both generation methods although their wall layouts appear to be different. The reduction of the users' throughput which was observed in a part of the simulations for the **[MLP]** wall layout is due to the greater probability that fewer obstacles will be located between the *Rx* and $iTx_{1\div3}$ compared to those between *Rx* and the *dTx*, which may result in increased interference (Fig. 1c). Conversely, the [**regular**] wall generation method provides roughly the same number of obstacles between users and the desired transmitter, and users and the interfering transmitters for each iteration (Fig. 1b).

V. Conclusion

In this work, simulation and analytical results for average wall attenuation and system-level simulation results evaluating the average users' throughput are presented. Ten scenarios are composed and investigated determined by four different wall layouts and two different transmitter locations.

The experimental results for average user throughput obtained via system-level simulations show the same trends as the SIR performance [2]. It transpires that, due to different wall arrangements, the average wall attenuation and average throughput are angularly dependent. When no walls are used, i.e. free space of signal propagation is taken into account, the specific transmitter arrangement does not influence the average throughput of the users.

The wall distribution models can be used to achieve more realistic indoor environments in order to test different techniques for interference mitigation. The closest to a real-world scenario is the **[RIEG]** wall arrangement method, which is realistic enough to be used as an indoor environment to test interference suppression techniques and algorithms for realistic human mobility and intelligent resource allocation.

References

[1] M. Müller, M. Taranetz, V. Stoynov, M. Rupp. "Abstracting Indoor Signal propagations: Stochastic vs. Regular", 58th International Symposium ELMAR-2016, Zadar, Sept. 2016, pp. 249-252.

[2] M. Müller, M. Taranetz, and M. Rupp, "Analyzing Wireless Indoor Communications by Blockage Models," in IEEE Access, Volume PP, Issue 99, Dec. 2016, .

[3] V. Stoynov. "Investigation of Indoor Wireless Communication Environment Using Abstract Modelling", E+E, vol. 52 No 1-2/2017, pp. 26-31.

[4] 3rd Generation Partnership Project (3GPP), "Evolved Universal Terrestrial Radio Access (E-UTRA); Further advancements for E-UTRA physical layer aspects," 3rd Generation Partnership Project (3GPP), TR 36.814, Mar. 2010.

[5] M. Rupp, S. Schwarz, and M. Taranetz, The Vienna LTE Advanced Simulators: Up and Downlink, Link and System Level Simulation, 1st ed., ser. Signals and Communication Technology. Springer Singapore, 2016.

[6] V. Stoynov, Z. Valkova-Jarvis, "The Impact of Abstract-Modelled Wall Layouts on User Throughput in Wireless Indoor Environments", First International Balkan Conference on Communications and Networking (BalkanCom 2017), Tirana, Albania, May 30-June 2, pp. 1-2.